

**Gamow-Teller decay population of  $^{64}\text{Ni}$  levels in the decay of  $1^+ ^{64}\text{Co}$** 

D. Pauwels,<sup>1,2</sup> D. Radulov,<sup>2</sup> W. B. Walters,<sup>3</sup> I. G. Darby,<sup>2</sup> H. De Witte,<sup>2</sup> J. Diriken,<sup>2</sup> D. V. Fedorov,<sup>4</sup> V. N. Fedosseev,<sup>5</sup> L. M. Fraile,<sup>6</sup> M. Huyse,<sup>2</sup> U. Köster,<sup>7</sup> B. A. Marsh,<sup>5</sup> L. Popescu,<sup>1</sup> M. D. Seliverstov,<sup>2,4</sup> A. M. Sjödin,<sup>8</sup> P. Van den Bergh,<sup>2</sup> J. Van de Walle,<sup>5</sup> P. Van Duppen,<sup>2</sup> M. Venhart,<sup>2,9</sup> and K. Wimmer<sup>10,11</sup>

<sup>1</sup>Belgian Nuclear Research Centre SCK•CEN, Boeretang 200, B-2400 Mol, Belgium

<sup>2</sup>Instituut voor Kern- en Stralingsfysica, KU Leuven, Celestijnenlaan 200D, B-3001 Leuven, Belgium

<sup>3</sup>Department of Chemistry and Biochemistry, University of Maryland, College Park, Maryland 20742, USA

<sup>4</sup>Petersburg Nuclear Physics Institute, RU-188300 Gatchina, Russia

<sup>5</sup>ISOLDE, CERN, CH-1211 Geneva 23, Switzerland

<sup>6</sup>Grupo de Física Nuclear, Universidad Complutense, CEI Moncloa, 28040 Madrid, Spain

<sup>7</sup>Institut Laue Langevin, 6 rue Jules Horowitz, F-38042 Grenoble Cedex 9, France

<sup>8</sup>KTH-Royal Institute of Technology, SE-10044 Stockholm, Sweden

<sup>9</sup>Slovak Academy of Sciences, SK-84511 Bratislava, Slovakia

<sup>10</sup>Physik Department E12, Technische Universität München, D-85748 Garching, Germany

<sup>11</sup>National Superconducting Cyclotron Laboratory, Michigan State University, East Lansing, Michigan 48824-1321, USA

(Received 24 September 2012; published 20 December 2012)

The  $^{64}\text{Co}$   $\beta$ -decay feeding levels in the well-studied  $^{64}\text{Ni}$  nucleus were investigated. Whereas the previously known  $^{64}\text{Co}$  decay scheme merely contained 2  $\gamma$  rays, the decay scheme established in this work contains 18, of which 5 are observed in this work and 6 were previously observed in an  $(n,\gamma)$  study but not placed in the  $^{64}\text{Ni}$  level scheme. Surprisingly, one additional level—placed at an excitation energy of 3578.7 keV—could be determined. The observed  $\beta$ -decay paths involve allowed  $\nu f_{5/2} \rightarrow \pi f_{7/2}$  and  $\nu p_{1/2} \rightarrow \pi p_{3/2}$  transitions. Three strongly fed levels around 4 MeV are interpreted to possess possible proton-intruder character.

DOI: [10.1103/PhysRevC.86.064318](https://doi.org/10.1103/PhysRevC.86.064318)

PACS number(s): 23.40.-s, 23.20.Lv, 21.10.-k, 27.50.+e

**I. INTRODUCTION**

Although the level structure of the stable  $^{64}\text{Ni}$  has been studied in detail through different reactions, the  $\beta$  decay of  $^{64}\text{Co}$  into  $^{64}\text{Ni}$  is poorly known [1]. The  $1^+$  spin and parity of the  $^{64}\text{Co}$  ground state has been demonstrated through  $(d,^2\text{He})$  reactions on  $^{64}\text{Ni}$  [2]. In particular, the principal configuration of that  $1^+$  ground state is thought to involve coupling of a single  $f_{5/2}$  neutron hole to a single  $f_{7/2}$  proton hole [2]. Hence, the decay is expected to involve a superallowed spin-flip transition in which an  $f_{5/2}$  neutron decays to fill the last remaining  $f_{7/2}$  proton hole. Direct  $\beta$ -decay population of the two lower  $2^+$  levels and a 90% ground-state to ground-state fraction were observed in a previously reported study of  $^{64}\text{Co}$   $\beta$  decay [1]. In this paper, a study of the decay of  $^{64}\text{Co}$  to levels of  $^{64}\text{Ni}$  is reported in which direct population of a number of additional low-spin levels is observed.

**II. EXPERIMENTAL DETAILS**

The  $^{64}\text{Co}$ -decay data were taken as part of a  $\beta$ -decay experiment of neutron-rich Mn isotopes at the CERN-ISOLDE facility. Pure and intense  $^{58,60-68}\text{Mn}$  ion beams were produced in three steps. First, the short-lived Mn isotopes were produced in an induced fission reaction of a 1.4-GeV proton beam impinging on a thick  $\text{UC}_x$  target (45 g/cm<sup>2</sup> thickness). Second, after diffusion out of the target and effusion of the reaction products into the ion source, the RILIS laser system [3] resonantly ionized the Mn atoms. The resonant laser ionization was realized by three Nd:YAG-pumped dye lasers. Third, the ions were accelerated over a 60-kV potential difference and

sent through the High Resolution Separator (HRS), where the isobars were separated according to their mass-over-charge value  $A/Q$ . In between the two HRS dipole magnets, slits were used to cut contaminant isobars which are easily ionized in the hot cavity as, for example,  $\text{Ga}^{1+}$ . Eventually, the Mn ion beam was implanted into a movable tape surrounded by three thin plastic  $\Delta E$   $\beta$  detectors and two MINIBALL  $\gamma$ -detector clusters [4]. Each detector signal was digitally read out by a free-running data-acquisition system storing its energy and time stamp based on a 40-MHz clock. A more detailed description of the detection setup can be found in Ref. [5].

With the HRS set to  $A/Q = 64$ , clean sources of  $^{64}\text{Mn}$  ( $T_{1/2} = 90$  ms) were obtained that, in turn, decayed to  $^{64}\text{Fe}$  ( $T_{1/2} = 2.0$  s). Subsequently,  $^{64}\text{Co}$  ( $T_{1/2} = 300$  ms) grew into equilibrium with the 2-s long-lived  $^{64}\text{Fe}$  parent providing a steady source for this study. Therefore, no new half-life value for  $^{64}\text{Co}$  could be obtained and the previous value of 300(30) ms from Ref. [1] was used. One part of the  $^{64}\text{Mn}$  data set was acquired with proton pulses and, thus,  $^{64}\text{Mn}$  implantations every 1.2 s, whereas a second part was obtained with proton pulses every 3.6 s. The implantation tape was moved at the end of every 39.6-s-long supercycle in order to remove long-lived daughter and contaminant activity.

Coincidence events and spectra presented in this article were obtained for the full counting period, whereas single events were analyzed after delays of 500 ms following each proton pulse during which time most of the 90-ms long-lived  $^{64}\text{Mn}$  has decayed to  $^{64}\text{Fe}$ . Hence, the data set used for the construction of the decay scheme included  $\gamma$  rays from both the decay of  $^{64}\text{Fe}$  ( $T_{1/2} = 2.0$  s) into levels of  $^{64}\text{Co}$  and the decay of  $^{64}\text{Co}$  ( $T_{1/2} = 300$  ms) to levels of  $^{64}\text{Ni}$ .

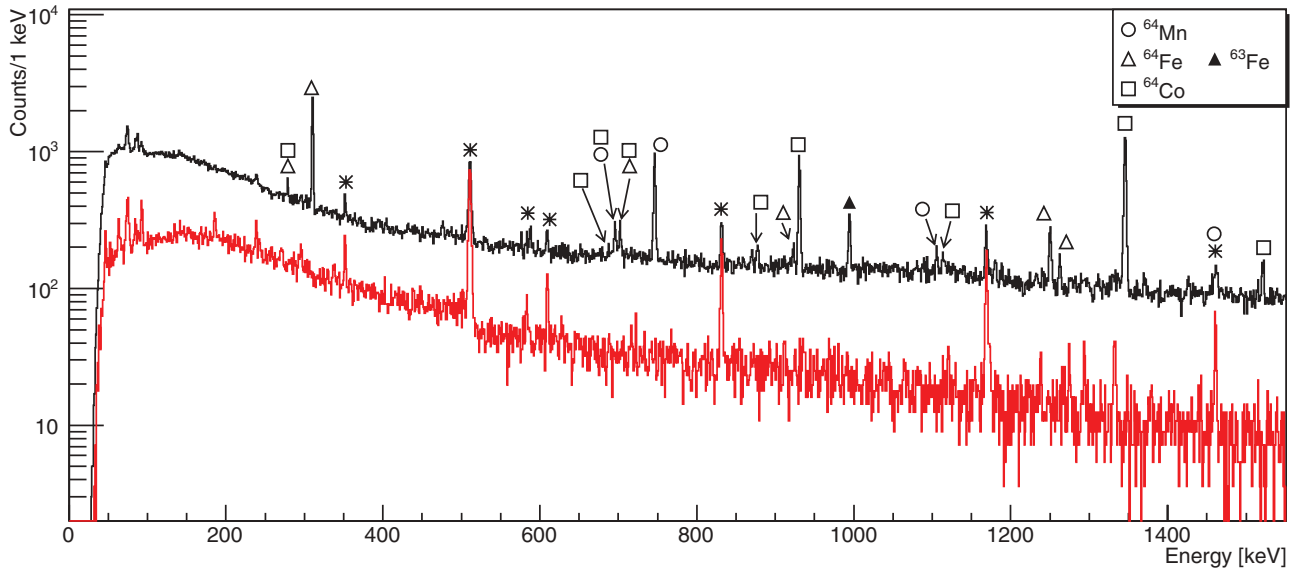


FIG. 1. (Color online) Spectra of single- $\gamma$  events later than 500 ms after each proton pulse with the lasers tuned to ionize Mn in black and with the lasers off normalized to the lasers-on time in red. Both spectra were taken in a cycle with proton pulses every 3.6 s representing only a subset of the total statistics. Lines following  $^{64}\text{Mn}$ ,  $^{64}\text{Fe}$ ,  $^{64}\text{Co}$ , and  $^{63}\text{Fe}$  decay are respectively marked according to the displayed legend. Contaminant and background lines are marked by a star.

In Fig. 1, the black single- $\gamma$  spectrum shows 2814 s of statistics out of the full 20 304 s for the purpose of direct comparison to the red time-normalized lasers-off spectrum, which represents identical experimental conditions. This comparison illustrates the purity level of the  $^{64}\text{Mn}$  ion beam. The

most important contaminants are singly charged  $^{64}\text{Ga}$ , which as a  $\beta^+$  emitter contributes to the 511-keV line, and doubly charged  $^{128}\text{In}^m/^{128}\text{Sn}^m$ . The  $(8^-)$   $^{128}\text{In}^m$  isomer  $\beta$ -decays to the  $(7^-)$  isomeric state of  $^{128}\text{Sn}$ , which subsequently decays to the ground state with a half-life of 6.5 s through a

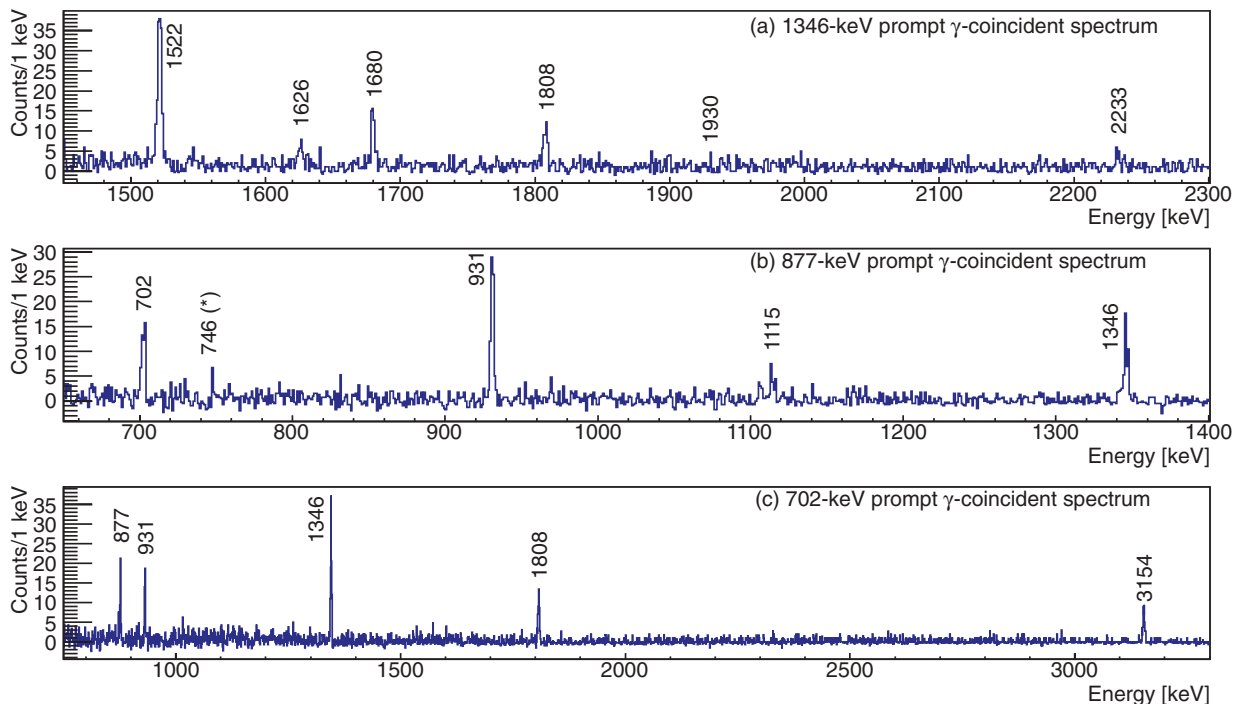


FIG. 2. (Color online) Selected background-subtracted coincidence gates for  $\gamma$  rays in the decay of  $^{64}\text{Co}$  to levels of  $^{64}\text{Ni}$ . (a) Gate on the 1346-keV  $\gamma$  ray; (b) gate on the 877-keV  $\gamma$  ray; (c) gate on the 702-keV  $\gamma$  ray. Coincident  $\gamma$  rays are indicated with their energy in keV. The 746-keV peak marked by a star in spectrum (b) is one bin wide and arises from a subtracted remnant of the intense  $2^+ \rightarrow 0^+$   $\gamma$ -ray transition in the  $^{64}\text{Mn}$  decay.

$(7^-) \rightarrow (4^+) \rightarrow 2^+ \rightarrow 0^+$   $\gamma$  cascade giving rise to  $\gamma$  lines at 91.1, 831.5, and 1168.8 keV, respectively.

### III. RESULTS

#### A. The $^{64}\text{Co}$ decay scheme

The new  $\gamma$  rays attributed to  $^{64}\text{Co}$  decay were selected on the basis of initial coincidences with the 931- and 1346-keV  $\gamma$  rays previously identified as depopulating the lower-energy  $2^+$  levels at 2277 and 1346 keV, respectively. Analysis of these coincidence gates indicated the further setting of coincidence gates on peaks at 279, 702, 877, 1115, 1522, 1808, 2233, and 3211 keV. Portions of the coincidence spectra that were scanned 500 ms after each proton pulse obtained by setting gates on the peaks at 702, 877, and 1346 keV are shown in Fig. 2. The energies, intensities, and placements of the  $\gamma$  rays attributed in this study to the decay of  $^{64}\text{Co}$  to levels of  $^{64}\text{Ni}$  are listed in Table I along with the observed  $\gamma$ -coincident peaks.

The decay scheme for  $^{64}\text{Co}$  is presented in Fig. 3. Of the 18  $\gamma$ -ray lines shown, the seven unmarked transitions with solid lines (black online) were previously established as depopulating levels identified in  $^{64}\text{Ni}$  following the  $^{63}\text{Ni}(n,\gamma)^{64}\text{Ni}$  reaction by Harder *et al.* [6]. Using coincidence evidence, six additional  $\gamma$  rays, marked by a rectangle (blue online), that were reported by Harder *et al.*, were placed in the level scheme. An additional five previously unidentified  $\gamma$  rays marked by a solid circle (red online) are identified in this study, although

some may have been observed in a study of the  $^{64}\text{Ni}(p,p'\gamma)$  reaction using a NaI(Tl) detector with 50-keV resolution [9].

Although 2922.1- and 3578.3-keV  $\gamma$  rays were observed in the  $^{63}\text{Ni}(n,\gamma)$  work [6] and would fit the  $4268.4 \rightarrow 1345.8$ - and  $3578.7 \rightarrow 0$ -keV transitions, respectively, no evidence of coincidence could be found in the present study. Therefore, they are not placed in the decay scheme. Nonetheless, the upper limits for their  $\gamma$  intensities (see Table I) do not rule out their placement.

The direct ground-state feeding was determined from a subset of the data which corresponds to the lasers-on and -off spectra of Fig. 1. The total number of  $^{64}\text{Mn}$   $\beta$  decays was deduced from the  $\beta$  counts during the 30-ms-long implantation period and the first 90 ms of the decay period, which corresponds to one half-life of  $^{64}\text{Mn}$  [10]. The background and contaminant activity was subtracted by the time-normalized laser-off data, while the longer-lived  $^{64}\text{Fe}$  ( $T_{1/2} = 2.0$  s) and  $^{64}\text{Co}$  ( $T_{1/2} = 0.3$  s) daughter activities were taken into account by extrapolating the  $\beta$  integral in the 35 ms preceding each implantation period with a 2-s single exponential function.

The  $^{64}\text{Mn}$   $\beta$ -delayed neutron branch into the  $A = 63$  decay chain is based on the peak integral of the 995-keV transition in  $^{63}\text{Fe}$  decay. The absolute 995-keV  $\gamma$  intensity of 43(8)% is deduced from the  $^{63}\text{Mn}$  data set [11]. Combined with the total number of  $^{64}\text{Mn}$  decays, this reveals a  $\beta$ -delayed neutron probability of 2.7(6)%, which is substantially smaller than the previous literature value of 33(2)% [12]. Iron and cobalt are refractory-type elements and, therefore, not expected to be directly present in the Mn ion beam. Hence, the

TABLE I. Energies, relative intensities, and placements of the  $\gamma$  rays observed in the decay of  $^{64}\text{Co}$  to levels of  $^{64}\text{Ni}$ . Where energy uncertainties are listed as 0.1 keV, those values were taken from Harder *et al.* The  $\gamma$  energies of coincident events are listed in the last column with the number of observed  $\gamma$ - $\gamma$  coincidences between brackets.

$E_\gamma$ (keV)	$I_{\text{rel}}$ (%)	Decaying-feeding level (keV)	$\gamma$ - $\gamma$ events (keV)(cts)
278.6(3)	0.6(3)	3856-3579	1346(44), 2233(44)
688.0(3)	0.5(2)	4268-3579	1346(15), 2233(11)
695.7(3)	0.8(3)	2972-2277	931(37), 1346(43)
702.2(3)	5.8(3)	3856-3154	877(77), 931(67), 1346(140), 1808(79), 3154(52)
877.2(1)	1.9(3)	3154-2277	702(76), 931(106), 1115(46), 1346(72)
930.8(1)	40.7(9)	2277-1346	696(48), 702(94), 877(117), 1346(1872)
1114.6(1)	2.3(4)	4268-3154	877(39), 931(30), 1346(53), 1808(19), 3154(18)
1345.8(1)	100	1346-0	279(45), 688(21), 696(43), 702(149), 877(87), 931(1868), 1115(55), 1522(243), 1626(32), 1680(90), 1808(68), 1930(7), 2233(17), 3211(23)
1521.6(1)	7.6(6)	2867-1346	1346(224)
1626.3(1)	1.0(4)	2972-1346	1346(24)
1680.1(1)	3.1(4)	3026-1346	1346(77)
1808.0(1)	2.4(4)	3154-1346	702(52), 1115(19), 1346(57)
1930.2(1)	0.3(2)	3276-1346	1346(6)
2232.9(1)	0.7(5)	3579-1346	279(41), 688(14), 1346(16)
2276.6(1)	<1	2277-0	
2922.1(1)	<0.5	4268-1346	
2972.0(1)	0.6(2)	2972-0	
3153.7(1)	3.3(6)	3154-0	702(58), 1115(15)
3210.5(4)	1.2(4)	4557-1346	1346(12)
3275.9(1)	2.2(5)	3276-0	
3578.3(1)	<0.3	3579-0	

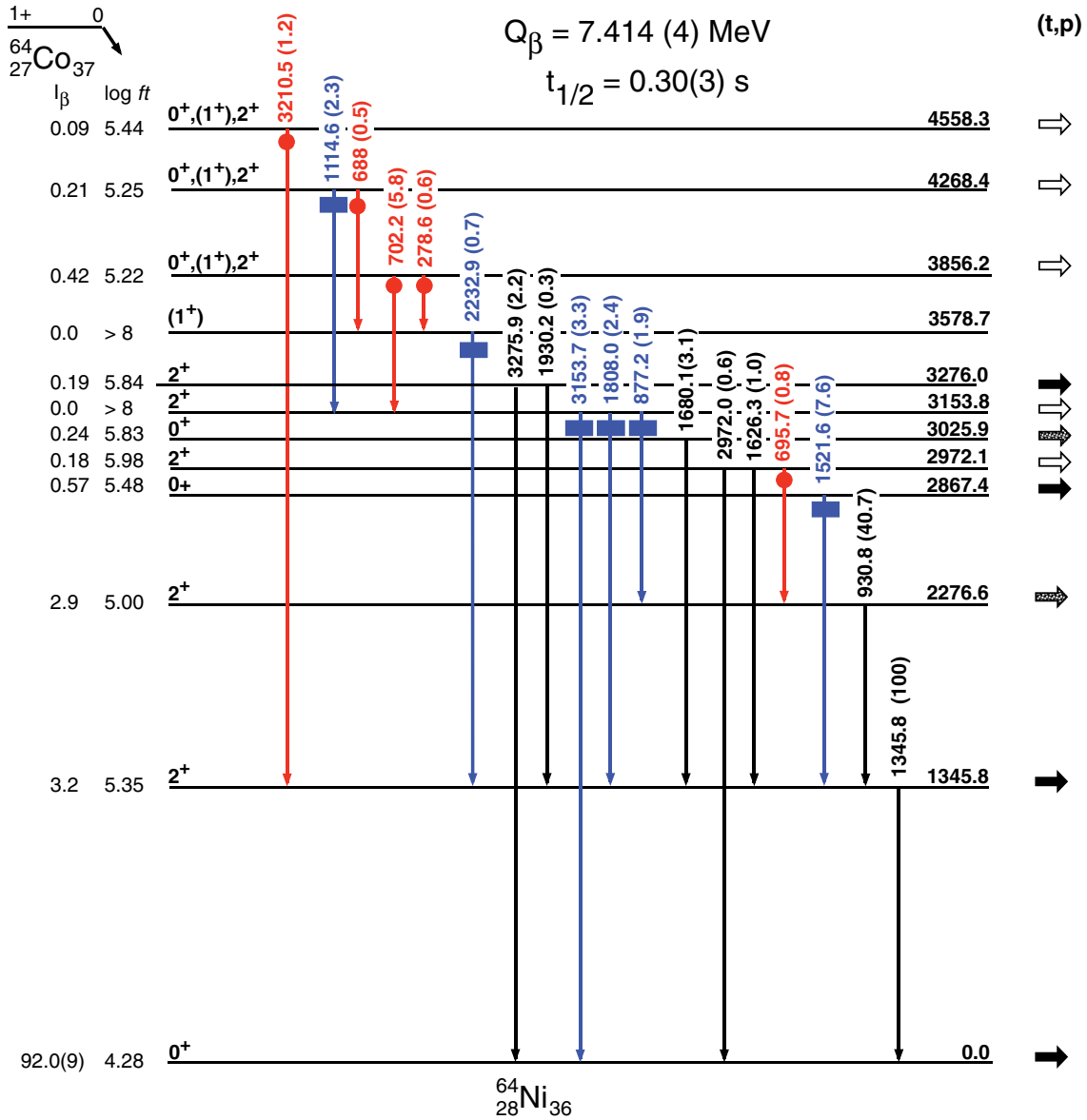


FIG. 3. (Color online) Decay scheme for 300-ms  $^{64}\text{Co}$  to levels of  $^{64}\text{Ni}$ . The seven  $\gamma$  rays with unmarked solid lines (black online) were observed and placed in the level scheme by Harder *et al.* in their study of the neutron-capture  $\gamma$  spectrum [6]. The six  $\gamma$  rays marked with a rectangle (blue online) were observed by Harder *et al.* but not placed in the level scheme. The five  $\gamma$  rays marked by a solid circle (red online) were observed in this study. The  $\beta$ -endpoint energy  $Q_\beta$  is taken from Refs. [7] and [8]. Levels with assigned spin and parity populated in the  $(t,p)$  reaction are shown with solid rightward-pointing arrows, whereas levels observed without spin and parity assignments are depicted by open rightward-pointing arrows. Half-filled arrows indicate that information from the  $(t,p)$  reaction was combined with this decay study to obtain spin assignments (see text).

total number of  $^{64}\text{Co}$  decays is 97.3(6)% of the total  $^{64}\text{Mn}$  decays. A cycle-correction factor was applied for the missing activity due to the tape move at the end of each 39.6-s-long supercycle.

Comparing the number of  $^{64}\text{Co}$  decays to the  $^{64}\text{Co}$   $\beta$ -delayed  $\gamma$  intensity leads to a direct ground-state branch of 92.0(9)%. This value is consistent with the 90(7)% value reported in the earlier  $\beta$ -decay work [1].

One goal of the present investigation is to identify which  $^{64}\text{Ni}$  levels are populated in the  $1^+ ^{64}\text{Co}$  decay and which are not. Actually, it turns out that the  $^{64}\text{Co}$  decay is not very

selective in its decay pattern to levels in  $^{64}\text{Ni}$ , as most of the previously known low-spin levels below 4600 keV are fed.

Levels populated in the  $^{62}\text{Ni}(t,p)^{64}\text{Ni}$  reaction [13] are indicated by horizontal arrows in Fig. 3. It can be seen that only the 3578.7-keV level was not fed in this reaction study. In fact, the level at 3578.7 keV is not only a remarkable one in the sense that it is established in this  $\beta$ -decay study, despite the detailed investigations of  $^{64}\text{Ni}$  through all the previous reactions like, for instance,  $(p,p'\gamma)$  [9], but also because it is observed through indirect  $\gamma$  decay from other levels that are populated in the  $\beta$  decay.

### B. Spin and parity assignments

Although transitions to many levels were reported in the  $(t,p)$  study, firm  $l$  values were only obtained for those transitions shown with closed arrows in Fig. 3. Nonetheless, the spin and parity assignments for the present decay scheme are strongly based on the selectivity of the  $(t,p)$  transitions. The allowed ones are those with natural parity and the angular distributions are sensitive to the respective  $l$  values. In  $^{62}\text{Ni}$ , which is a thoroughly studied nucleus with a similar structure as the one of  $^{64}\text{Ni}$ , none of the unnatural transitions to  $1^+$ ,  $2^-$ , and  $3^+$  levels nor transitions to  $1^-$  levels are observed in the  $(t,p)$  [13] or  $(p,t)$  [14] reactions. Instead, most  $0^+$  and all  $2^+$  levels ( $<4$  MeV) are populated. Some  $4^+$  levels are weakly populated and one  $3^-$  level is strongly populated.

With the above selection rules for the  $^{62}\text{Ni}(t,p)^{64}\text{Ni}$  study, the spin and parities for the respective levels populated in the  $^{64}\text{Co}$  decay can be assigned as follows.

The 2276.6-keV level is assigned  $2^+$ , despite the fact that no direct ground-state transition was observed in the present study. The upper limit of 1% for the relative intensity of the 2276.6-keV transition is listed in Table I. The  $(t,p)$  data suggest  $0^+$  or  $2^+$ . The population from a  $3^-$  level, however, which was not observed in the present study but established by Ref. [15], rules out  $0^+$ . Nonetheless, a  $0^+$  doublet may be present within  $\pm 15$  keV.

The 2876.4-keV level is  $0^+$  based on the  $(t,p)$  angular distribution.

A  $2^+$  spin and parity is assigned for the 2972.1-keV level. The fact that it directly decays to the  $0^+$  ground state rules out  $0^+$  and the high cross section in  $(t,p)$  rules out a spin  $J = 1$ .

Like the 2876.4-keV level, the 3025.9-keV level is  $0^+$  based on the  $(t,p)$  angular distribution even though  $L = 0$  was only tentatively assigned in Ref. [13].

The 3158-keV  $(t,p)$  level is a doublet of the 3153.8- and 3166.1-keV states, of which the latter is known to be  $4^+$ . Because the  $(t,p)$  angular distribution is intermediate between  $L = 2$  and  $L = 4$  and  $0^+$  can be ruled out because of the ground-state transition, the 3153.8-keV level is assigned a spin and parity of  $2^+$ .

The 3276-keV level is known to be  $2^+$ .

The upper three levels at 3856.2, 4268.4, and 4558.3 keV are strongly  $\beta$ -fed from the  $1^+$   $^{64}\text{Co}$  ground state. Because these levels are also populated in  $(t,p)$ ,  $0^+$  or  $2^+$  spin and parities are suggested.

The 3578.7-keV level established in this work is an interesting one. The nonobservation in the  $(t,p)$  study and the observed decay to the first-excited  $2^+$  level restrict the possible spin and parities to  $J = 1$ ,  $2^-$ , and  $3^+$ . However, also  $1^-$  and  $2^-$  can be disregarded because  $E1$  transitions from the positive-parity 3856.2- and 4268.4-keV levels would not be able to compete with their  $M1$  and/or  $E2$  transitions to the  $2^+$  level at 3153.8 keV. Finally, one can consider that if the 3578.3-keV transition observed in the  $(n,\gamma)$  reaction were to be the direct ground-state transition, then only a  $1^+$  assignment remains possible. Therefore, we tentatively assign the 3578.7-keV level a spin and parity of  $(1^+)$ . Note that this would be the only proposed  $1^+$  level which does not appear to be directly populated in  $\beta$  decay.

Examination of the decay scheme reveals that all of the known  $0^+$  and  $2^+$  levels below 3.5 MeV are observed, but the  $2^+$  level at 3154 keV does not seem to be directly populated via  $\beta$  decay. Both of the excited  $0^+$  levels identified in the  $(t,p)$  reaction are populated with less than 1% of the intensity. Between 3.5 and 5 MeV, six additional  $2^+$  levels were identified in the  $(t,p)$  reaction, none of which are observed in the decay of  $^{64}\text{Co}$ .

### IV. DISCUSSION

One aim of this study was to examine the  $\beta$  decay of the  $1^+$  ground state of  $^{64}\text{Co}$  to permit comparison with decay in adjacent nuclides.  $^{64}\text{Co}$  is the lightest odd-odd Co nucleus with a clear  $1^+$  ground state with a proposed ground-state configuration of  $\pi f_{7/2}^{-1} \otimes \nu f_{5/2}^{-3}$  whose configuration is strongly supported by the strong population in the  $^{64}\text{Ni}(d,^2\text{He})$  reaction.

The principal decay path is likely to be the direct decay of the single odd  $f_{5/2}$  neutron to fill the last remaining  $f_{7/2}$  proton hole, leaving the nucleus in the ground state of  $^{64}\text{Ni}$ . An alternate decay path would involve decay of one of the paired  $f_{5/2}$  neutrons to fill the last  $f_{7/2}$  hole state, leaving the nucleus with two unpaired  $f_{5/2}$  neutrons. Although these two unpaired  $f_{5/2}$  neutrons can couple to both spin 2 and spin 4, direct  $\beta$  decay from the  $1^+$  ground state of  $^{64}\text{Co}$  is possible only to the  $2^+$  configuration. These two mechanisms are the main decay paths leading to  $0^+$  and  $2^+$  end configurations.  $^{64}\text{Co}$  directly decays to all known  $0^+$  and  $2^+$   $^{64}\text{Ni}$  levels below 3.5 MeV. Their observed decay strengths then would indicate the amount of (un)paired  $\nu f_{5/2}$  mixing in the respective  $0^+$  and  $2^+$  levels.

The surprisingly low  $\log ft$  values for population of the three levels at 3856, 4368, and 4558 keV, whose depopulation is largely via  $2-\gamma$  cascades, suggest a different  $\beta$ -decay pathway. The  $\log ft$  values indicate an allowed transition that could arise from decay of the  $p_{1/2}$  neutron into the  $p_{3/2}$  proton orbital across the  $Z = 28$  closed shell. The schematic description for this decay process would involve

$$\begin{aligned} & [(\pi \mathbf{f}_{7/2})^{-1} \cdot (\nu p_{3/2})^4 \cdot (\nu p_{1/2})^2 \cdot (\nu f_{5/2})^2 \cdot (\nu \mathbf{f}_{5/2})^1]_{1^+} \\ & \rightarrow [(\pi \mathbf{f}_{7/2})^{-1} \cdot (\pi \mathbf{p}_{3/2})^{+1} \cdot (\nu p_{3/2})^4 \cdot (\nu \mathbf{p}_{1/2})^1 \\ & \quad \cdot (\nu f_{5/2})^2 \cdot (\nu \mathbf{f}_{5/2})^1]_{2^+}, \end{aligned}$$

where the unpaired orbitals are shown in bold, and the decaying  $p_{1/2}$  nucleon is underlined. These levels would involve both a broken neutron pair and a broken proton pair. Hence, their  $\gamma$  decay via a two-step transition would be consistent with the “re-pairing” of first one of the broken pairs, and then the other. The presence of particle-hole intruder structures in this energy range was identified via strong  $L = 3$  pickup strength in the  $^{65}\text{Cu}(d,^3\text{He})^{64}\text{Ni}$  reaction [16]. Because of the suggested proton-intruder character of the 3856-, 4368-, and 4558-keV states, they could serve as a test bench for a large-scale shell-model assessment with, e.g., the Lenzi-Nowacki-Poves-Sieja (LNPS) interaction [17].

As discussed in Sec. III B, the 3578.7-keV level established in this work is the only candidate for a possible  $1^+$  level. Remarkably, it is not directly  $\beta$  fed, but through the  $\gamma$  decay



of the suggested proton intruders at 4368 and 4558 keV. The fact that it is not observed in other reactions like  $(t,p)$  [13],  $(e,e')$  [18],  $(n,n')$  [19], or  $(p,p'\gamma)$  [9] underlines its unique configuration among the other low-energy states in  $^{64}\text{Ni}$ .

## V. CONCLUSIONS

The  $\beta$  decay of 300-ms  $1^+$   $^{64}\text{Co}$  to levels of  $^{64}\text{Ni}$  was investigated and largely extended in comparison to the former  $\beta$ -decay study. A rather unselective decay to previously known  $0^+$  and  $2^+$  levels and a dominant direct ground-state feeding with a  $\log ft$  of 4.3 is observed. Important  $\beta$  strength to levels near 4 MeV was established, which could indicate a proton particle-hole character of their configurations. A new

level at an excitation energy of 3578.7 keV could be placed with a tentative spin and parity of  $1^+$ , pointing to a unique configuration.

## ACKNOWLEDGMENTS

Support is acknowledged from FWO-Vlaanderen (Belgium), GOA/2004/03 (BOF-KU Leuven), the Interuniversity Attraction Poles Programme—Belgian State—Belgian Science Policy (BriX network P7/12), the European Commission within the Sixth Framework Programme through I3-EURONS (Contract No. RII3-CT-2004-506065), the U.S. Department of Energy, Office of Nuclear Physics, under Grant No. DEFG02-94-ER40834, and the Spanish MINECO through Grant No. FPA2010-17142.

- 
- [1] V. Rahkonen and J. Kantele, *Phys. Fenn.* **9**, 103 (1974).  
 [2] L. Popescu *et al.*, *Phys. Rev. C* **75**, 054312 (2007).  
 [3] V. N. Fedosseev *et al.*, *Rev. Sci. Instrum.* **83**, 02A903 (2012).  
 [4] J. Ebert *et al.*, *Prog. Part. Nucl. Phys.* **46**, 389 (2001).  
 [5] D. Pauwels *et al.*, *Nucl. Instr. Meth. Phys. Res. B* **266**, 4600 (2008).  
 [6] A. Harder *et al.*, *Z. Phys. A* **343**, 7 (1992).  
 [7] R. Ferrer *et al.*, *Phys. Rev. C* **81**, 044318 (2010).  
 [8] G. Audi, A. H. Wapstra, and C. Thibault, *Nucl. Phys. A* **729**, 337 (2003).  
 [9] P. Beuzit, J. Delaunay, J. P. Fouan, and N. Cindro, *Nucl. Phys. A* **128**, 594 (1969).  
 [10] <http://www.nndc.bnl.gov/ensdf/>  
 [11] D. Radulov (private communication).  
 [12] M. W. Hannawald, Ph.D. thesis, Johannes Gutenberg Universität, Mainz, 2000 (unpublished).  
 [13] W. Darcey, R. Chapman, and S. Hinds, *Nucl. Phys. A* **170**, 253 (1971).  
 [14] D. H. Kong-A-Siou and H. Nann, *Phys. Rev. C* **11**, 1681 (1975).  
 [15] T. Pawlat *et al.*, *Nucl. Phys. A* **574**, 623 (1994).  
 [16] G. Heymann and P. M. Cronje, *Nucl. Phys. A* **193**, 357 (1972).  
 [17] S. M. Lenzi, F. Nowacki, A. Poves, and K. Sieja, *Phys. Rev. C* **82**, 054301 (2010).  
 [18] M. R. Braunstein, J. J. Kraushaar, R. P. Michel, J. H. Mitchell, R. J. Peterson, H. P. Blok, and H. de Vries, *Phys. Rev. C* **37**, 1870 (1988).  
 [19] Y. G. Kosyak, D. K. Katpov, and L. V. Chekushina, *Bull. Acad. Sci. USSR Phys. Ser.* **53**, 68 (1989).